Available online at www.sciencedirect.com
SCIENCE DIRECT®
PERGAMON
Polyhedron 22 (2003) 1183–1189
POLYHEDRON
www.elsevier.com/locate/poly

NMR and UV spectra of lanthanide decatungstates $LnW_{10}O_{36}^{n-}$ and $W_{10}O_{32}^{4-}$: a study of some peculiarities in spectra by the extended Hückel MO method

M. Inoue [a], T. Yamase [a,*], L.P. Kazansky [b]

[a] Research Laboratory of Resource Utilization, Tokyo Institute of Technology, 4259 Nagatsuta, Midori-ku, Yokohama 226-8503, Japan
[b] Institute of Physical Chemistry, Russian Academy of Sciences, 31 Leninski pr., 117071 Moscow, Russia

Received 7 October 2002; accepted 6 January 2003

Abstract

The decatungstates for Eu, Tm, Yb and Lu have been synthesized, and ^{183}W and ^{17}O NMR spectra have been measured for their solutions. The latter three compounds may be formed in the solid state but in aqueous solution they are practically completely decomposed. ^{183}W NMR and UV spectra of the polyoxotungstates have been analyzed by extended Hückel molecular orbital calculations. The calculated HOMO–LUMO separation for $LaW_{10}O_{36}^{9-}$, $Ce^{IV}W_{10}O_{36}^{8-}$, $W_{10}O_{32}^{4-}$ and $W_6O_{19}^{2-}$ corresponds to the wavelength of the lowest charge transfer band observed in UV spectra of aqueous solutions. Using the calculated energy of MOs for $LaW_{10}O_{36}^{9-}$, $Ce^{IV}W_{10}O_{36}^{8-}$, $W_{10}O_{32}^{4-}$ and $W_6O_{19}^{2-}$, it was found that the general trend in the change of the ^{183}W NMR chemical shifts depends on the paramagnetic contribution which is determined by the excited states. The ^{183}W chemical shifts is shown to linearly depend on the sum of five inverse energy separations between bonding MOs involving W5d-orbitals and five antibonding W5d*-orbitals for the nucleus under consideration. It is also shown that the charges on tungsten atoms do not play an important role in the change of the chemical shift.

Keywords: Polyoxotungstate; ^{183}W and ^{17}O NMR shifts; EHMO calculations

1. Introduction

Since the first X-ray single-crystal structure studies of $Ce^{IV}W_{10}O_{36}^{8-}$ and $U^{IV}W_{10}O_{36}^{8-}$ have appeared [1,2], there have been numerous publications on the crystal structures of a large number of lanthanide decatungstate (LDT) complexes [3] and their spectroscopic properties [4–7]. Quite recently, it was shown that some of them are catalytically active. LDTs containing La–Yb can catalyze the oxidative reaction of both cyclooctene to epoxycyclooctane and benzyl alcohol to benzaldehyde in the presence of hydrogen peroxide [8]. It is noteworthy that structure determinations are limited to the Pr–Er series and other LDTs have not been X-ray crystallographically analyzed. Moreover, there are some unusual peculiarities in both ^{17}O and ^{183}W NMR spectra which are still unclear. So, studies have been extended to attempt to prepare LDTs for the rest of the lanthanide series and to get more insight into the nature of NMR chemical shifts and the bonding in these complexes. The data will be compared with hexatungstate ($W_6O_9^{2-}$) and decatungstate ($W_{10}O_{32}^{4-}$), whose structures resemble LDT, by means of NMR, UV and IR spectroscopies and extended Hückel molecular orbital (EHMO) calculations.

2. Experimental

All $LnW_{10}O_{36}^{n-}$ complexes have been synthesized according to known procedures [4] and characterized by spectroscopic methods. The number of water molecules in the solid has been determined by thermogravimetric analysis. IR spectra have been recorded as KBr

* Corresponding author. Tel.: +81-45-924-5260; fax: +81-45-924-5276.
E-mail address: tyamase@res.titech.ac.jp (T. Yamase).

0277-5387/03/$ - see front matter © 2003 Elsevier Science Ltd. All rights reserved.
doi:10.1016/S0277-5387(03)00119-0

pellets on a JASCO FT/IR-5000 spectrometer with main strong peaks observed for $Na_9EuW_{10}O_{36}\cdot 32H_2O$ at 940, 843, 783, 704, 542, 414 cm^{-1}, $Na_9YbW_{10}O_{36}\cdot 22H_2O$—936, 847, 783, 708, 545, 489, 420 cm^{-1}, $Na_9TmW_{10}O_{36}\cdot 76H_2O$—935, 835, 777, 703, 499, 418 cm^{-1} and for $Na_9LuW_{10}O_{36}\cdot 51H_2O$—935, 844, 786, 540, 497, 421 cm^{-1}. The elemental analyses have been performed by the ICP-AES method on a RIGAKU SPECTRO CIROS CCD: for $Na_9EuW_{10}O_{36}\cdot 32H_2O$, Obsd: Na, 5.9; Eu, 4.1; W, 54.9, Calc.: Na, 6.2; Eu, 4.5; W, 54.9%; for $Na_9TmW_{10}O_{36}\cdot 76H_2O$, Obsd: Na, 5.4; Tm, 6.4; W, 61.0, Calc.: Na, 5.0; Tm, 4.1; W, 44.2%; for $Na_9YbW_{10}O_{36}\cdot 22H_2O$, Obsd: Na, 4.2; Yb, 5.8; W, 56.6, Calc.: Na, 6.5; Yb, 5.4; W, 57.6% and for $Na_9LuW_{10}O_{36}\cdot 51H_2O$, Obsd: Na, 6.3; Lu, 4.5; W, 51.2, Calc.: Na, 5.6; Lu, 4.7; W, 49.5%. UV spectra of the aqueous solutions have been measured on a Hitachi 330 spectrometer. NMR spectra have been recorded on a JEOL GSX-500 NMR spectrometer at 20.7 MHz for the ^{183}W nucleus and at 67.70 MHz for the ^{17}O nucleus at natural abundance. The chemical shifts are measured relative to Na_2WO_4 solution for ^{183}W spectra and water for ^{17}O spectra.

CACHe software has been used for EHMO calculations with the parameters [9] given in Table 1.

Crystallographic data of polyoxotungstates used for EHMO calculations are taken from the corresponding published X-ray structure determinations. Despite very close structural similarity among all studied complexes, some small changes in the geometric characteristics result in notable differences in UV and NMR spectra and they will be considered in detail.

3. Results and discussion

Earlier, ^{183}W and ^{17}O NMR spectra have been published [6] for all LDTs with the exception of Eu and lanthanides at the end of the series—Tm, Yb and Lu. The structures have been solved by X-ray crystallography practically for all lanthanides from Pr(III) to Er(III) [3]. The structure of $LnW_{10}O_{36}^{n-}$ is built from two mono-lacunary moieties derived from the highly symmetrical Lindquist anion $W_6O_{19}^{2-}$. The four-terminal oxygen atoms left from removal of W=O form a square antiprism around the Ln cation (Fig. 1).

Table 1
CACHe parameters used for EHMO calculations

Nucleus	Orbital	Ionization potential (eV)	Coefficient	Exponent
W	5d	9.000	1.000	2.577
	6p	3.969	1.463	
	6s	8.000	1.741	
O	2p	13.620		2.018
	2s	28.480		2.192

Hückel parameter: 1.75, basis STO-3G.

All LDTs are characterized by two lines in ^{183}W NMR spectra with the ratio of 4:1 corresponding to two types of tungsten atoms in the structure (Fig. 1). For diamagnetic LDTs with the exception of $Ce^{IV}W_{10}O_{36}^{8-}$, the two lines are closely spaced in the range from +5 to −20 ppm with the more intense line observed at lower field. However, due to paramagnetism of most lanthanides, the ^{183}W NMR spectra undergo substantial change depending on the magnetic properties of Ln^{3+} and the chemical shift may attain ±2000 or more ppm.

It is clearly seen in the ^{183}W NMR spectrum of $EuW_{10}O_{36}^{9-}$ (Table 2), where the two lines are widely apart, due to the interaction of the f-electrons through the oxygen bridges, the line assigned to eight tungsten atoms is substantially shifted to high field. The presence of two lines with the ratio of 4:1 confirms that the structure of LDT in solution corresponds to the one found in the crystalline state.

The second confirmation of the existence of the structure in solution may be obtained from the ^{17}O NMR spectra (Fig. 1(b)). Due to paramagnetism, the line assigned to the oxygen atoms O_f forming a square antiprism around Eu is observed at high field. Other lines may be assigned to different types of oxygen atoms

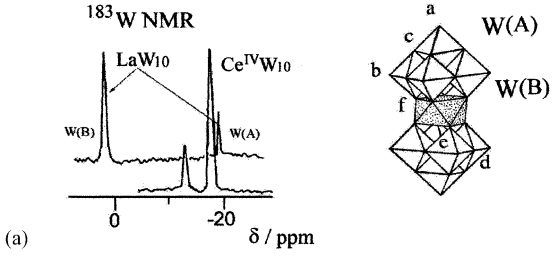

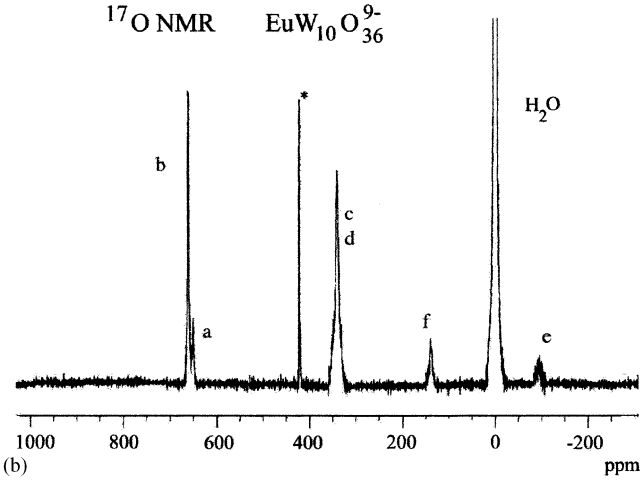

Fig. 1. (a) Structure of $LnW_{10}O_{36}^{n-}$, ^{183}W spectra for $LaW_{10}O_{36}^{9-}$ and $Ce^{IV}W_{10}O_{36}^{8-}$; (b) ^{17}O NMR spectrum of $EuW_{10}O_{36}^{9-}$ (* denotes admixture of WO_4^{2-}).

Table 2
The chemical shifts of ^{183}W and ^{17}O NMR spectra of $LnW_{10}O_{36}^{n-}$ and polyoxotungstates

Ln	W(A)	W(B)	O_a	O_b	O_c	O_d	O_e	O_f
Ce^{IV}	−13	−18	662	679	361	344	−32	616
Eu	−18	−611	652	667	350	332	−94	139
Lu	20	−4	649	672	356	352	?	507
Tm	−90	−86						
Yb	82	8	650	670	374	362	?	?
$W_6O_{19}^{2-}$ [a]	58		772	413			−81	
$W_{10}O_{32}^{4-}$ [a]	−165	−45	761	430	421	416	−47	
$W_7O_{24}^{6-}$ [a]	258, −86, −171		650	627	597	314	296	257 70

[a] Taken from published data [10].

in the structure of $EuW_{10}O_{36}^{9-}$. The position of the line corresponding to O_f substantially depends on the magnetic properties of the lanthanide cation [6,7]. As usual the most deshielded oxygen atoms are the terminal ones, with the most intense lines assigned to the terminal oxygen atoms O_b bound to the tungsten atoms W(B) located in the two square arrays (Fig. 1). The weak line shifted to higher field is assigned to the terminal oxygen atoms (O_a) linked to apical tungsten atoms W(A).

Concerning the other LDTs, analysis of IR spectroscopic data points out that solid Lu, Tm and Yb complexes synthesized according to a known procedure with an excess tungsten content form the decatungstate structure. However, solutions of these complexes reveal complex patterns, and in general observed lines in both ^{17}O and ^{183}W NMR spectra can be assigned to $W_7O_{24}^{6-}$ (Table 2) [10]. The other lines may be assumed to be due to the complexes of $LnW_{10}O_{36}^{9-}$. It seems surprising but in contrast to these decatungstates, the smallest Lu^{3+} cation forms stable complexes with the bulky lacunary heteropolyanions such as $PW_{11}O_{39}^{7-}$ and even with $P_2W_{17}O_{61}^{10-}$ in aqueous solution [11,12]. According to NMR data, these complexes do not reveal degradation upon dissolution in water. Attempts to change the conditions (varying pH or adding organic solvent) have not resulted in stabilization of these LDTs, as described by other groups. It seems that such small cations with charge 3+ cannot stabilize the lacunary W_5O_{18}, which is unknown in the free state in solution (see, e.g., the lanthanide contraction throughout a series of $LnW_{10}O_{36}^{9-}$ decreasing the bond length Ln–O_f from 2.48 Å for PrO_8 to 2.40 Å for DyO_8 [3]. In contrast, Ce(IV) forms an LDT [1] even though it has small ionic radius with its bond distance Ce–O_f equal to 2.38 Å). On the other hand, lacunary Keggin and Dawson anions, which are stable in aqueous solution, easily interact with small Ln cations.

One of the most intriguing points in ^{183}W NMR spectra of the diamagnetic $LnW_{10}O_{36}^{n-}$, which reveal a two-line pattern with an intensity ratio of 4:1 with the more intense line corresponding to deshielded tungsten (B), is the inversion of the pattern that is observed for $Ce^{IV}W_{10}O_{36}^{8-}$ (Fig. 1(a)). The apical tungsten atoms W(A) for $Ce^{IV}W_{10}O_{36}^{8-}$ are slightly deshielded (−13 ppm) compared to W(B) (−18 ppm) located in square arrays. This suggests some changes in the electronic structure of these decatungstates probably due to a subtle difference in the geometric characteristics of the polyoxoanions. It should be mentioned that the ^{183}W NMR spectrum of $W_{10}O_{32}^{4-}$, whose structure resembles LDT, also markedly differs from those of LDT. Two lines with 4:1 pattern are notably shifted to high field and are widely spaced. Besides, $W_{10}O_{32}^{4-}$ is characterized by the hypsochromic shifting of the CT band observed in the UV spectrum compared both with $W_6O_{19}^{2-}$ and LDT. Because both UV spectra and NMR chemical shifts of the anion are derived from its electronic structure, there should be a correlation of the observed chemical shift and its anionic structure. In order to understand these differences in NMR spectra as well as in UV spectra of decatungstates, we have used EHMO calculations which have been carried out for these large polyoxotungstates.

Considering UV spectra it is relevant to compare some experimental data where drastic changes in UV spectra occur when going from $W_6O_{19}^{2-}$ to $W_{10}O_{32}^{4-}$. Due to a change of the structure (two types of tungsten atoms) and formation of the linear bonding W–O–W, the lowest charge transfer (LCT) band previously observed at 275 nm for $W_6O_{19}^{2-}$ is split into at least two bands for decatungstate, one being observed at 325 nm and other one at 250–260 nm (Fig. 2(a)). These bands may roughly characterize LCT transitions of $O \rightarrow W_b$ and $O \rightarrow W_a$ due to two different tungsten atoms. It should be noted that the formation of the linear bonding W_b–O–W_b between two halves in the $W_{10}O_{32}^{4-}$ anion may be assumed to be responsible for such red-shifting when compared with the UV spectrum of the $W_6O_{19}^{2-}$ anion.

As for LDT, UV spectra do not correspond to only one band at 260 nm (seen as an extended shoulder on the most intense absorption band) (Fig. 2(b)) and should be decomposed into (at least) two Gaussian curves. They may correspond to two transitions of $O \rightarrow W(B)$ and $O \rightarrow W(A)$ in both types of octahedra-like we have suggested for $W_{10}O_{32}^{4-}$. We can suppose that the LCT band corresponds to the transition from oxygen atoms to tungsten W(B) and therefore due to the similarity of UV spectra for all lanthanides (Ln^{3+}), the pattern of the electronic transitions will be similar. In contrast to it, the shoulder is observed in the UV spectrum of $Ce^{IV}W_{10}O_{36}^{8-}$ at 330 nm, which is responsible for the coloring (light orange) of this complex. This shoulder may be explained by a low-energy CT band involving excitation from non-bonding orbitals of O_f to the Ce 3f-orbital.

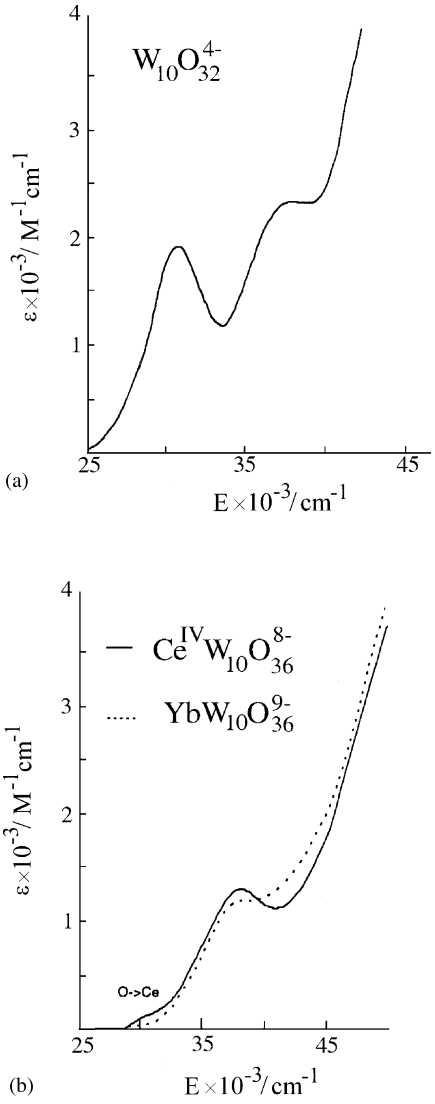

Fig. 2. UV spectra of (a) $W_{10}O_{32}^{4-}$ and (b) $YbW_{10}O_{36}^{9-}$ and $Ce^{IV}W_{10}O_{36}^{8-}$.

In order to understand some peculiarities in UV and NMR spectra, we have tried to analyze them by using EHMO calculations. The ab initio method has been usually used to analyze the NMR chemical shifts for small and simple molecules [13]. However, the use of the ab initio method for the calculation of the chemical shifts for large molecules (particularly the ones having a nucleus such as ^{183}W) seems to present a cumbersome problem, especially if a relativistic correction is needed. Therefore, the calculations of the chemical shifts by the ab initio method are restricted to quite simple molecules. We hope to use a rather simple method to analyze the NMR chemical shifts for the large molecules. The results of the calculation of the electronic structure by EHMO method have been successfully used to analyze the chemical shifts of ^{183}W, ^{95}Mo and ^{17}O NMR spectra for octahedral fragments of polyoxoanions [14,15]. Recently, it has been shown that EHMO method gives a similar result to the ab initio method for the fragments of polyoxometalates and successfully explains the trend in the chemical shift of ^{183}W NMR spectra of various polyoxotungstates [16].

It has been shown in the literature [14,15] that the metal chemical shifts linearly correlate with the sum of the inverse energy difference between the averaged energy of the bonding and five antibonding molecular orbitals involving W5d-orbitals. However, the calculations have been made for isolated octahedra that constitute polyoxoanions and in this case the five antibonding MOs are composed mainly of W5d*-orbitals of a single metal atom. But in polyoxoanions, each W5d-orbital of several metal atoms is used in many both bonding and antibonding MOs whose energies spread over a large range. In our approach, we choose one specific (apical- or square-positioned) tungsten atom and construct an MO diagram reducing molecular orbitals to five antibonding W5d*-orbitals by means of calculating a baricenter of each orbital (picking them out of from a large number of antibonding MOs) using the coefficients of atomic orbitals involved in molecular orbitals and their energies. By this way we have found the baricenters of five atomic W5d*-orbitals of this specific atom (chosen from two apical or eight of two square sets) that contributes to the antibonding MO formed by all participating tungsten atoms (Table 3).

In Fig. 3 for comparison the MO diagrams for $W_{10}O_{32}^{4-}$ and $LaW_{10}O_{36}^{9-}$ representing only antibonding MOs (orbitals from 129 to 178) are given. The calculations show the position of the bonding MOs and their narrow spread do not change much for the polyoxotungstate anions under consideration and therefore they are not shown. Once again, by using the energy of the bonding MO and W5d atomic orbital coefficients of the corresponding atom, we have calculated an "effective" energy of the bonding MO involving only W5d-orbitals from which the excitation of the electron takes place. This "effective" energy will be used for calculations of the energy separations between bonding and antibonding MOs.

The most interesting point for $W_{10}O_{32}^{4-}$ is that the lowest unoccupied molecular orbital (LUMO) is formed by W5d-orbitals lying in a plane perpendicular to the terminal W=O bonds of eight tungsten atoms of B-type and this non-generate MO is fairly separated from other antibonding MOs (Fig. 3). From this, we may conclude that LCT band observed at $\sim$30 kK should be attributed to the excitation of electrons from the non-bonding highest occupied MO (HOMO) consisting mainly of 2p-orbitals of bridging oxygen atoms to this LUMO. The HOMO–LUMO separation for $W_6O_{19}^{2-}$ in the MO diagram is larger corresponding to lower wavelength in comparison with the one of $W_{10}O_{32}^{4-}$ (Table 4).

Table 3
Energy (ae) of baricenters of antibonding W5d* orbitals, Λ and ^{183}W NMR chemical shifts for polyoxotungstates

Anion	$LaW_{10}O_{36}^{9-}$		$CeW_{10}O_{36}^{8-}$		$W_{10}O_{32}^{4-}$		$W_6O_{19}^{2-}$
	W(A)	W(B)	W(A)	W(B)	W(A)	W(B)	W
$d_{x^2-y^2}$	0.1262	0.0816	0.1198	0.1068	0.1172	0.0558	0.1362
d_{z^2}	0.0547	0.0275	0.0392	0.0013	0.0578	0.0342	0.0782
d_{xz}	−0.2119	−0.1957	−0.2149	−0.1931	−0.1829	−0.1766	−0.2071
d_{yz}	−0.2119	−0.2188	−0.2149	−0.2200	−0.1829	−0.2061	−0.2071
d_{xy}	−0.2440	−0.2389	−0.2442	−0.2347	−0.2426	−0.2528	−0.2577
d_{bond}	0.5199	0.5188	0.5190	0.5194	0.5247	0.5204	0.5156
Λ (e V^{-1})	0.4927	0.4960	0.4988	0.4937	0.4656	0.4905	0.4991
δ (ppm)	−19	2	−12	−17	−165	−45	58

For $W_{10}O_{32}^{4-}$, the second CT band is probably due to the excitation of the electrons from the HOMO to the MO involving W5d$^*_{xy}$-orbitals of the apical tungsten atoms and with partially admixture of W(B) 5d-orbitals.

To consider the ^{183}W NMR chemical shifts for large polyoxotungstates, we have used the same approach based on EHMO calculations as described in a previous study [13]. As known, the chemical shift is understood in terms of the shielding of the nucleus by circulating electrons derived from the applied magnetic field. The shielding consists of two components—diamagnetic (σ_{dia}) and paramagnetic (σ_{para}) [14,15]. The first one, σ_{dia}, depends on the ground state and is related to the electron density at the nucleus in question. The diamagnetic contribution is easily calculated and may be found in tables [17]. Usually it does not change much for closely related molecules. The second one, σ_{para}, results from the mixing of small fractions of electronic excited-state wave functions with the ground state. Generally for the metal NMR, the shielding of the nucleus is dominated by the paramagnetic shielding. It can be calculated by sophisticated methods like ab initio [14] or by DFT (density functional theory) methods [18]. The dominating contribution of the excited states into the paramagnetic shielding is confirmed by linear correlations of the chemical shifts and wavelength of the LCT for polyoxoanions with similar structures [19,20]. By using simplified formula relating the paramagnetic shielding and the excited states:

$$\sigma_{para} = K \sum \{1/(E_b - E_a)\} \quad (1)$$

where K is the product of constants and $(E_b - E_a)$ is the energy difference between bonding and antibonding MOs, it was also found that ^{183}W and ^{95}Mo NMR chemical shifts linearly correlated with the sum of the five inversed energy separations, Λ ($= \Sigma\{1/(E_b - E_a)\}$), between the bonding MO and five antibonding MOs both involving metal atomic orbitals calculated for isolated polyhedrons MO_n of a large number of polyoxoanions [13], thus corresponding to the Md → Md* transitions.

The MO diagrams for a large polyoxotungstate are rather complex and we should apply some approximations in order to extract information from the calculated values. So, we have in mind to reduce such a diagram to a more simplified one. From the calculated energies of the antibonding MOs, the baricenters of five atomic orbitals have been found (Fig. 3(a)) for two types of tungsten atoms. Two reduced MO diagrams show a substantial difference in the positions of orbitals for different tungsten atoms (W(A) and W(B)) and the sums $\Sigma\Delta E^{-1} = \Lambda$ of five inverse energy separations (i.e., the difference between the "effective" energy E_d of the averaged bonding MO as mentioned above, and the energy E_{d*} of five antibonding MOs, i.e., d_{xy}, d_{xz}, d_{yz}, d_{x^2}, d_{z^2} and $d_{x^2-y^2}$) have been calculated. Previous calculations for the individual WO_n polyhedron have shown that increasing Λ results in larger paramagnetic shielding with the resonance line observed at low field and consequently it corresponds to a more positive ^{183}W chemical shift [13].

According to our estimation of Λ for $W_{10}O_{32}^{4-}$, the value of Λ is larger for tungsten atoms W(B) corresponding to higher chemical shift in comparison with W(A), thus in general confirming our approach in treatment of the chemical shifts. Moreover, the calculated Λ for $W_6O_{19}^{2-}$ is larger than both values for $W_{10}O_{32}^{4-}$ (Table 3), again completely corresponding to the correlation between Λ and chemical shifts.

Concerning MO calculations for $LaW_{10}O_{36}^{9-}$, we have used the structural data of $PrW_{10}O_{36}^{9-}$ [3] as the closest analog of the former and data for $CeW_{10}O_{36}^{8-}$ [1]. The former MO diagram (only antibonding MOs are presented excluding 4f-orbitals, which are located between the HOMO and LUMO (No. 152) involving W5d-orbitals) is shown in Fig. 3.

The same approach as described above for reducing all MOs to a bonding MO W5d with an "effective" energy, from which the electron is excited to five main antibonding W5d*-orbitals for two types of tungsten atoms, has been used and the results are presented in Fig. 3 and Table 3. Similar to $W_{10}O_{32}^{4-}$, the different

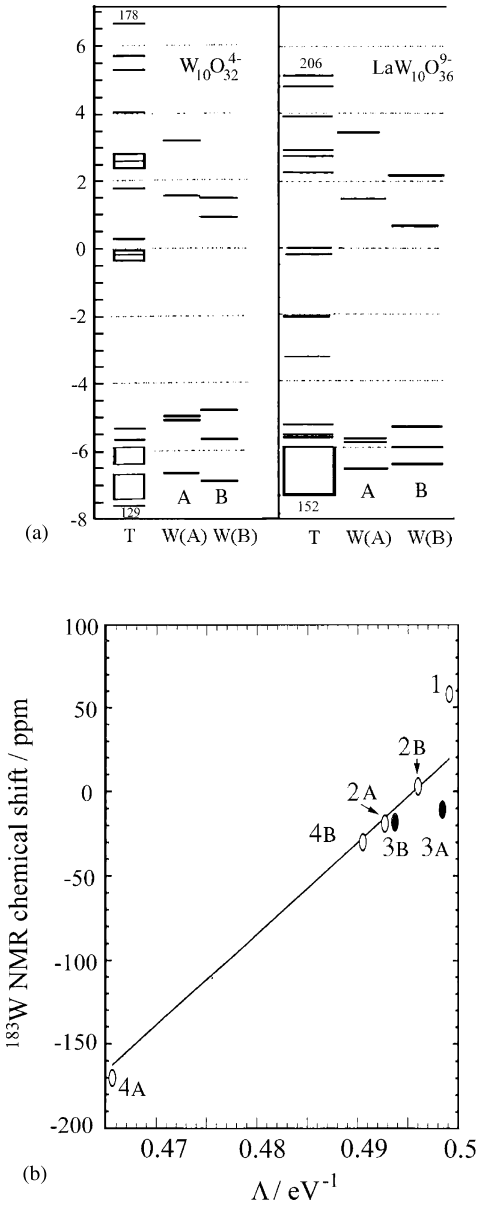

Fig. 3. (a) MO diagrams for $W_{10}O_{32}^{4-}$ and $LaW_{10}O_{36}^{9-}$ (only antibonding levels are presented) (boxes mean closely spaced MOs). (b) Plot between calculated Λ and observed ^{183}W NMR chemical shifts for polyoxotungstates: (1) $W_6O_{19}^{2-}$, (2) $LaW_{10}O_{36}^{9-}$, (3) $Ce^{IV}W_{10}O_{36}^{8-}$ and (4) $W_{10}O_{32}^{4-}$.

calculated Λ values for $LaW_{10}O_{36}^{9-}$ also reflect the difference in the electronic structure of the two types of tungsten atoms and consequently the difference in the chemical shifts of the two types of tungsten atoms, giving a lesser Λ value for the apical tungsten and therefore its line is shifted to high field. This is fully consistent with the previously found trend in the ^{183}W NMR chemical shifts. However, for $CeW_{10}O_{36}^{8-}$ the chemical shift pattern is reversed. In this case, we have found that the calculated Λ becomes larger for the apical tungsten atom, corresponding to larger chemical shift.

Taking into account these correlations and Eq. (1), we have compared the ^{183}W NMR chemical shifts with the calculated Λ values for different types of tungsten atoms in four polyoxoanions $W_6O_{19}^{2-}$ (1), $W_{10}O_{32}^{4-}$ (4), $LaW_{10}O_{36}^{9-}$ (2), $CeW_{10}O_{36}^{8-}$ (3) (Fig. 3(b)). Linear correlation clearly shows the importance of the paramagnetic contribution to the chemical shift and gives explanation of the reverse pattern in the ^{183}W NMR spectra of $CeW_{10}O_{36}^{8-}$. Moreover, reducing the large number of antibonding molecular orbitals to the five basic W5d-orbitals has proved to be a useful approach for understanding the nature of the chemical shifts when large polyoxoanions are considered.

The EHMO method is enabling the calculation of the charges on atoms in molecule as well, and there are some attempts to correlate the NMR chemical shifts with the electronic population on the nucleus under consideration [13,14,21]. However, it was argued that the charge on atoms does not play an important role in the change of the chemical shift. Despite some ambiguities in calculating the charge on atoms by using EHMO method, we have tried to plot the ^{183}W NMR chemical shifts against the calculated charges on tungsten atoms in different polyoxoanions (Fig. 4(a)). Though there is

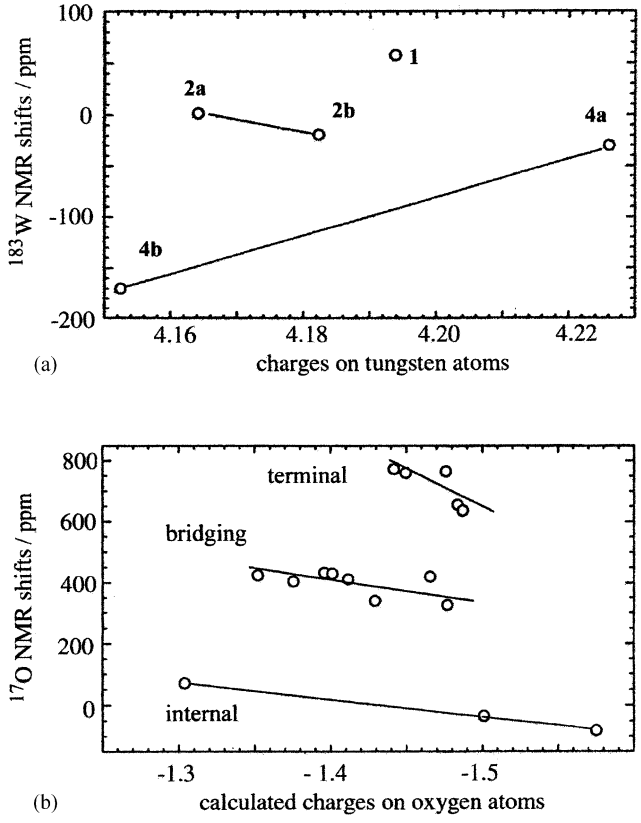

Fig. 4. (a) Plot between calculated charges on tungsten atoms and ^{183}W NMR chemical shifts; (b) plot between calculated charges on oxygen atoms and the ^{17}O NMR chemical shifts.

Table 4
Calculated energy gap O–W and LCT wavelength of polyoxotungstates

Anion	$E_{O\rightarrow W(B)}$ (eV) calculated	$E_{O\rightarrow W(A)}$ (eV) calculated	LCT (obs), nm wavelength
$W_6O_{19}^{2-}$	5.303		275
$W_{10}O_{32}^{4-}$	4.767	5.768	317
$LaW_{10}O_{36}^{9-}$	5.657	5.763	250

no clear-cut correlation between the two parameters, a general tendency is slightly seen to show deshielding of the nucleus upon decreasing the electron population.

The same thing may be said relatively for ^{17}O NMR chemical shifts (Fig. 4(b)). For different types of oxygen atoms—terminal, bridging or internal—the dependence of the chemical shifts upon charge on the given atom is observed. However, there is no direct relation of the charge with the chemical shift.

4. Conclusion

In this work, attempts to synthesize decatungstates for heavy lanthanides have been undertaken. Unfortunately in aqueous solutions, these decatungstates decompose forming heptatungstate. The stable $EuW_{10}O_{36}^{9-}$ has, however, been obtained and its ^{183}W and ^{17}O NMR spectra are measured. By means of calculations of the electronic structure of LDT, $W_{10}O_{32}^{4-}$ and $W_6O_{19}^{2-}$ by using EHMO method, the differences in the ^{183}W NMR and UV spectra are discussed and explained. It is shown that even subtle changes in geometric parameters of the polyoxoanions result in marked variations of the spectroscopic properties and in the calculated parameters of the electronic structure. It is also important to underline that application of EHMO method for large anions and interpretation of the calculated data may give better understanding of the electronic structure of the polyoxoanions and the influence of geometry on the spectroscopic data. Despite some limitations, the results of the EHMO calculation may be rather valuable help in studying polyoxometalates.

Acknowledgements

L.P.K. is very grateful to the JSPS fellowship and the possibility to carry out this study during 1997–1998.

References

[1] J. Iball, J.N. Low, T.J.R. Weakley, J. Chem. Soc., Dalton Trans. 10 (1974) 2021.
[2] (a) A.M. Golubev, L.P. Kazansky, E.A. Torchenkova, L.A. Muradian, V.I. Simonov, V.I. Spitsyn, Dokl. SSSR 221 (1975) 351;
(b) A.M. Golubev, L.P. Kazansky, E.A. Torchenkova, L.A. Muradian, V.I. Simonov, V.I. Spitsyn, Koord. Khim. 3 (1977) 920.
[3] T. Ozeki, T. Yamase, Acta Crystallogr. B 50 (1994) 128.
[4] R.D. Peacock, T.J.R. Weakley, J. Chem. Soc. A 11 (1974) 1836.
[5] L.P. Kazansky, A.M. Golubev, I.I. Baburina, E.A. Torchenkova, V.I. Spitsyn, Izvestia Akad. Nauk SSSR, Ser. Khim. (1978) 2215.
[6] M.A. Fedotov, E.P. Samokhvalova, L.P. Kazansky, Polyhedron 15 (1996) 2241.
[7] R. Shiozaki, A. Inagaku, A. Nishino, E. Nisio, M. Maekawa, H. Kominami, Y. Kera, J. Alloys Compd. 234 (1996) 193.
[8] R. Shiozaki, A. Inagaku, A. Nishino, E. Nisio, M. Maekawa, H. Kominami, Y. Kera, J. Alloys Compd. 261 (1997) 132.
[9] CACHe, Oxford Molecular Group, Inc., 1996.
[10] (a) R.I. Maksimovskaya, K.G. Burtseva, Polyhedron 4 (1985) 1559;
(b) J.J. Hastings, O.W.J. Howarth, J. Chem. Soc., Dalton Trans. (1992) 209;
(c) O. Gansow, R.K.C. Ho, W.G. Klemperer, J. Organomet. Chem. 87 (1980) 27.
[11] M.A. Fedotov, B.Z. Pertsikov, D.K. Danovich, Polyhedron 9 (1990) 1249.
[12] (a) J. Bartis, M. Dankova, M. Blumenstein, L.C. Frankensconi, Inorg. Chem. 35 (1996) 1497;
(b) J. Bartis, S. Sukal, M. Dankova, E. Kraft, R. Kronzon, M. Blumenstein, L.C. Francesconi, J. Chem. Soc., Dalton Trans. (1997) 1937.
[13] L.P. Kazansky, P. Chaquin, M. Fournier, G. Herve, Polyhedron 17 (1998) 4653.
[14] (a) H. Nakatsuji, in: J.A. Tossel (Ed.), Nuclear magnetic shielding and Molecular Structure. NATO ASI Series, Reidel, Doedrecht, 1993;
(b) H. Nakatsuji, M. Sugimoto, S. Saito, Inorg. Chem. 29 (1990) 1221, 3095.
[15] C.J. Jameson, H.S. Gutovsky, J. Chem. Phys. 40 (1964) 1714.
[16] L.P. Kazansky, P. Chaquin, M. Fournier, G. Herve, Polyhedron 17 (1998) 4353.
[17] G. Malli, C. Froese, Int. J. Quant. Chem. 1 (1967) 793.
[18] V.G. Malkin, O.L. Malkina, E. Casida, D.R. Salahub, J. Am. Chem. Soc. 116 (1994) 5898.
[19] L.P. Kazansky, Koord. Khim. 3 (1977) 327.
[20] R. Acerete, C.F. Hammer, L.C.W. Baker, J. Am. Chem. Soc. 104 (1982) 5384.
[21] M. Bühl, W. Thiel, U. Fleisher, W. Kutzelnigg, J. Phys. Chem. 99 (1995) 4000.